

# Nucleating a metastable quantum phase transition

Oleksandr Fialko<sup>1</sup>, Marie-Coralie Delattre<sup>1</sup>, Joachim Brand<sup>1</sup> and Andrey R. Kolovsky<sup>2,3</sup>

<sup>1</sup>*Centre for Theoretical Chemistry and Physics and New Zealand Institute for Advanced Study, Massey University, Private Bag 102904 NSMC, Auckland 0745, New Zealand*

<sup>2</sup>*Kirensky Institute of Physics, 660036 Krasnoyarsk, Russia and*

<sup>3</sup>*Siberian Federal University, 660041 Krasnoyarsk, Russia*

(Dated: December 2, 2024)

Finite topological quantum systems can undergo continuous metastable quantum phase transitions to change their topological nature. Here we show how to nucleate the transition between ring currents and dark soliton states in a toroidally trapped Bose-Einstein condensate. An adiabatic passage to wind and unwind its phase is achieved by explicit global breaking of the rotational symmetry. This could be realized with current experimental technology.

Phase transitions have long been considered equilibrium phenomena of infinite systems that can involve interesting non-equilibrium nucleation dynamics, e.g. the formation of topological defects [1]. In recent years, quantum phase transitions have also been identified in excited states [2–5] by the nonanalytic change in spectral properties, or their finite-system precursors, as a system parameter is changed. Such phase transitions are not obtained in equilibrium but they have dynamical consequences [3, 4]. So far, little is known about the nucleation process.

Nucleation of equilibrium quantum phase transitions often relies on external symmetry breaking, which can occur *locally*. An example is the Ising model [6], where a tiny external magnetic field is needed for breaking the rotational symmetry of the spins and allowing the system to equilibrate. Similar mechanism were discussed in the context of vortex nucleation in Bose gases [7–9]. Here we theoretically investigate the quantum phase transition between metastable states of a Bose gas in a toroidal trap identified in Ref. [5]. The metastable states are the yrast states for  $N$  atoms, states of minimal energy with given angular momentum  $J = lN\hbar$ . In particular these are vortex states, where  $l$  is integer, which correspond to a ring current. When the toroidal trap is rotated about its axis, the ground state jumps between vortex states [10] and thus  $l$  is a topological charge. A continuous quantum phase transition occurs between excited vortex states and metastable yrast states with noninteger  $J/(N\hbar)$ , which are approximated by dark solitons in mean field theory. Dark solitons have a localised density notch [11] and thus locally break rotational symmetry in addition to changing the topological nature of the system, although no symmetry breaking is required for the phase transition in the quantum description of the finite system.

In this Letter, we show how to nucleate the phase transition by means of a *global* symmetry breaking potential, which creates an adiabatic passage through metastable states. The relevance of global symmetry breaking in contrast to the local symmetry breaking mechanisms known in equilibrium phase transitions [1, 2, 6] suggest that this nucleation process is restricted to finite systems.

The global symmetry breaking is achieved by tilting the trap axis by some angle  $\theta$  and rotating it with the frequency  $\Omega$ . The frequency  $\Omega$  is decreased from a maximum value  $\Omega_{max}$  to a minimum value  $\Omega_{min}$  within a finite time interval, after which the tilt is decreased (see Fig. 1). Under certain conditions for the parameters, which will be identified later, angular momentum is established in the Bose gas up to a dark soliton state ( $J/N\hbar \approx 0.5$ ) or a vortex state ( $l = 1$ ). The protocol is counterintuitive and reminiscent of the stimulated Raman adiabatic passage used in quantum optics to populate a metastable state through an intermediate level by a counterintuitive pulse sequence [12].

Interacting bosonic atoms of mass  $m$  confined to a rotating toroidal trap are described by the Hamiltonian  $\hat{H} = \int_0^L dx \hat{\Psi}^\dagger \hat{\mathcal{H}} \hat{\Psi}$  with

$$\hat{\mathcal{H}} = -\frac{\hbar^2}{2m} \frac{\partial^2}{\partial x^2} + \frac{U}{2} \hat{\Psi}^\dagger \hat{\Psi} + \epsilon \cos\left(\frac{2\pi}{L}x - \Omega t\right), \quad (1)$$

where  $\hat{\Psi} \equiv \hat{\Psi}(x)$  is the atomic field operator,  $U$  the bare interaction constant assumed repulsive ( $U > 0$ ), and  $\epsilon = mgR \sin(\theta)$  the strength of the symmetry breaking potential (where  $mg$  is the gravitational force). The toroidal trap is approximated by a one-dimensional ring of the length  $L = 2\pi R$ .

Let us first discuss the outlined problem in the mean-field approximation. Using a rotating coordinate frame with frequency  $\Omega$  and introducing the scaled variables  $\phi = x/R$ ,  $\tau = tE_0/\hbar$ ,  $\omega = \hbar\Omega/(2E_0)$ , the Gross-Pitaevskii (GP) equation reads

$$i \frac{\partial \chi}{\partial \tau} = \left[ -(\partial_\phi - i\omega)^2 + 2\pi \frac{\gamma}{E_0} |\chi|^2 + \frac{\epsilon}{E_0} \cos(\phi) \right] \chi, \quad (2)$$

where  $\gamma = U(N-1)/L$  and  $E_0 = \hbar^2/(2mR^2)$  gives the relevant energy scale. The classical field  $\chi$  is normalized as  $\int_0^{2\pi} |\chi|^2 d\phi = 1$  and it is periodic on  $\phi$ ,  $\chi(0) = \chi(2\pi)$ . We apply Broyden's method [13] to solve Eq. (2) numerically for the stationary solutions  $\chi(\tau, \phi) = \chi(\phi)e^{-i\mu\tau}$ , where  $\mu E_0$  is the chemical potential. For  $\epsilon = 0$  we present in Fig. 2(a) three solutions corresponding to two vortex

states  $\chi(\phi) = e^{il\phi}/\sqrt{2\pi}$  with  $l = 0$  and  $l = 1$ , which are connected by a soliton branch. Finite  $\epsilon$  opens a gap in the soliton branch, see Fig. 2(b). The lower branch corresponds to a soliton sitting on the crest, while the upper branch connects to a soliton located in the trough of the external potential. In the following we will show that the lower branch is dynamically unstable, while the upper branch is stable. Thus an adiabatic passage through the upper branch is possible. Direct numerical simulation of the system dynamics on the basis of Eq. (2) confirms this expectation. The solid lines in the middle and lower panels in Fig. 1 show the momentum per atom as a function of time for the adiabatic protocols indicated in the upper panel. A vortex and a soliton are formed, respectively. The symmetry breaking dark soliton profile is shown in the inset.

We proceed with discussing the necessary conditions for an adiabatic passage. Useful insight into the physics of the considered process is obtained within a two-mode approximation, which is justified for small  $\gamma \ll E_0$ . Neglecting all coefficients in the Fourier expansion except  $k = 0, 1$  of the function  $\chi$ ,  $\chi(\tau, \phi) = \sum_k b_k(\tau) \exp(ik\phi)$ , the system dynamics is described by the effective Hamiltonian

$$H_{cl} = E_0(1 - 2\omega)I + \gamma I(1 - I) + \epsilon \sqrt{I(1 - I)} \cos \vartheta, \quad (3)$$

where  $I = |b_1|^2$  and  $\vartheta$  is the relative phase for the amplitudes  $b_0$  and  $b_1$ . The phase portrait of (3) contains a stability island around the elliptic point  $(I, \vartheta) = (I^*, 0)$ , where  $I^*$  depends on  $\omega$  and is  $I^* = 1/2$  for  $\omega = 1/2$  and close to zero and unity for  $\omega = 1$  and  $\omega = 0$ , respectively.

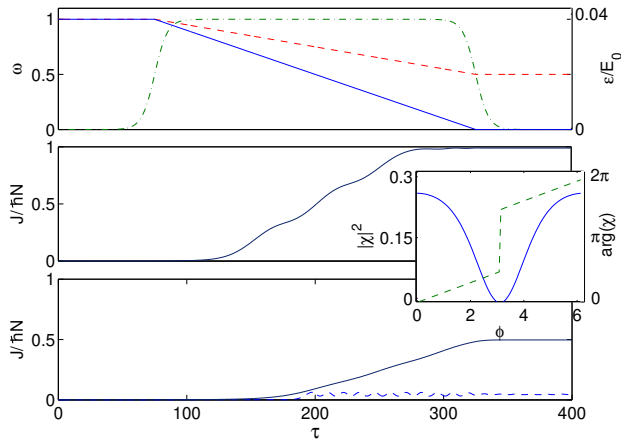


FIG. 1. Adiabatic passage from the ground to the vortex (middle panel) and the dark soliton (lower panel) states. The upper panel shows the protocol for variations of the perturbation parameter  $\epsilon$  (dash-dotted line) and the precession frequency  $\omega$  (solid and dashed lines) for  $\gamma = 0.8E_0$ . Inset: The dark soliton state. Full line represents its density, dashed line represents its phase.

We note that in the lab frame this stability island corresponds to a nonlinear resonance. Thus the adiabatic passage has a simple physical interpretation: by ramping  $\epsilon$  to a finite value we capture the system into the nonlinear resonance, transport it to any desired value of  $I$  by adiabatically changing the frequency  $\omega$  from  $\omega_{max}$  to  $\omega_{min}$ , and release the system by ramping  $\epsilon$  back to zero. The necessary condition for the time scale of this process is  $\Delta t \gg \Omega_s^{-1}$ , where  $\Omega_s \approx \sqrt{\gamma\epsilon}/\hbar$  is the frequency of small oscillations near the elliptic point of the stability island (the approximate sign is replaced by an equal sign for  $\omega = 1/2$ ).

For stronger nonlinearity,  $\gamma > E_0$ , when the two-mode approximation is not justified, the adiabaticity conditions and stability can be studied using the Bogoliubov approach, which linearizes the time dependent GP equation (2) [11]. This leads to the eigenvalue problem

$$\begin{aligned} \lambda_i u_i &= (\hat{H}_{GP} - \mu + 2\pi\gamma/E_0|\chi|^2)u_i + 2\pi\gamma/E_0\chi^2 v_i, \\ -\lambda_i v_i &= (\hat{H}_{GP} - \mu + 2\pi\gamma/E_0|\chi|^2)v_i + 2\pi\gamma/E_0\chi^{*2} u_i \end{aligned} \quad (4)$$

Here,  $\chi = \chi_\omega(\phi)$  is the stationary solution for the upper soliton branch in Fig. 2(d) and  $\hat{H}_{GP}$  is given in the square brackets in Eq. (2). For the lower branch we find a single imaginary eigenvalue  $\lambda$ , which indicates that the solutions on this branch are dynamically unstable [11]. The Bogoliubov analysis for the upper branch shows that it is dynamically stable and that there is a gap to the lowest lying elementary excitation. The corresponding frequency  $\Omega_s = \lambda E_0/\hbar$  has the asymptotic behavior

$$\Omega_s = \begin{cases} \sqrt{\gamma\epsilon}/\hbar & , \gamma \ll E_0 \\ \sqrt{E_0\epsilon}/\hbar & , \gamma \gg E_0 \end{cases} \quad (5)$$

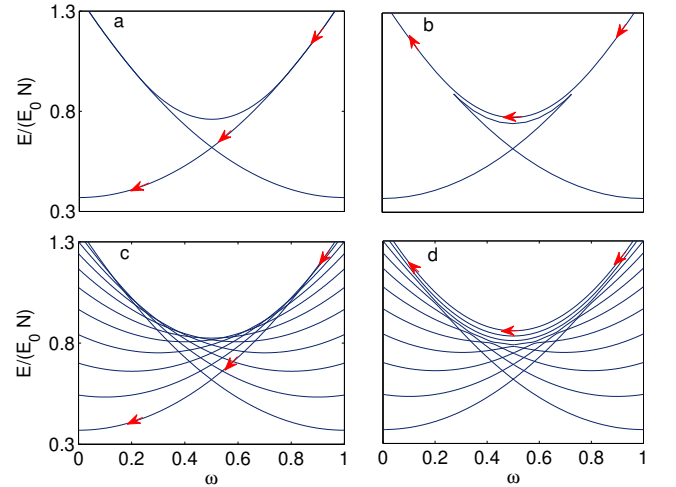


FIG. 2. The energy of the GP equation (upper row) and the energy spectrum of the Hamiltonian (9) in the 2-modes approximation (lower row). Parameters are  $\gamma = 0.8E_0$ , and  $\epsilon = 0$  (left column) and  $\epsilon = 0.04E_0$  (right column). The arrows show the passage under adiabatic change of the frequency  $\omega$ .

For small nonlinearities  $\gamma \ll E_0$  this result agrees with the previous two-mode analysis.

The large  $\gamma$  result can be understood by noting that the soliton is a localized object. In this case  $\Omega_s$  is interpreted as the frequency of small oscillations of the soliton around a stationary point. The energy of a soliton can be approximately calculated as

$$\frac{E_s}{N} \approx \frac{8}{3} \hbar n c \left(1 - \frac{u^2}{c^2}\right)^{3/2} + \frac{\gamma}{2\pi R} + \frac{\hbar^2 v_b^2}{m R^2}, \quad (6)$$

where  $v_b = 1/2 - 2\hbar\Omega/E_0$ ,  $u = R[E_0/\hbar - \Omega - \partial\phi_s/\partial t]$  [11]. By assuming that the energy of the soliton is a conserved quantity and using the local density approximation  $c^2 = \gamma n(\phi_s)/2m$ , where the density at the position  $\phi_s$  of the soliton is modulated by the external potential, we arrive at

$$m \left( \frac{\partial\phi_s}{\partial t} \right)^2 \pm \frac{\epsilon}{2R^2} \phi_s^2 \approx \text{const}, \quad (7)$$

which is valid for  $\Omega \approx E_0/\hbar$ . The  $\pm$  sign corresponds to a soliton sitting at the trough or the crest of the external potential, respectively. While the minus sign describes an unstable situation (lower soliton branch in Fig. 2b), the plus sign describes harmonic oscillations of a particle with mass  $2m$  [14]. The soliton is thus dynamically stable, with the frequency of small oscillations  $\Omega_s = \sqrt{\epsilon/(2mR^2)} = \sqrt{E_0\epsilon}/\hbar$ .

In practice, the adiabaticity condition  $\Delta t \gg \Omega_s^{-1}$  discussed above should be made even stronger. We found that during the excitation process it is practically impossible to avoid oscillations of the dark soliton around the equilibrium position. The amplitude of such oscillations should be smaller than the healing length. By equating the force exerted on the soliton by external potential,  $m_s \Omega_s^2 R \phi_s$ , with the inertial force caused by accelerating frame,  $m_s R \dot{\Omega}$ , we find the displacement of the soliton relative to the center of the external potential,  $R \phi_s = R \dot{\Omega} / \Omega_s^2$ . Then the requirement that this displacement is smaller than the healing length  $\xi = \sqrt{\hbar^2/2m\gamma}$  results in the following condition

$$\frac{\partial\Omega}{\partial t} \ll \frac{\xi}{R} \frac{E_0\epsilon}{\hbar^2}. \quad (8)$$

The numerical simulation of the system dynamics confirms the estimate (8). For the parameters of Fig. 1 the right hand side of (8) is  $\approx 0.04(E_0/\hbar)^2$ . It is seen in Fig. 1 that for  $\dot{\Omega} = 0.04(E_0/\hbar)^2$  the adiabatic condition is not met (blue dashed line), while for a ten times smaller rate  $\dot{\Omega} = 0.004(E_0/\hbar)^2$  the dark soliton and the vortex states (black solid lines) are reached. In the middle panel one also sees the mentioned small oscillations of the soliton.

The mean-field analysis presented so far can be substantiated by a quantum analysis. Using scaled variables,

a rotating coordinate frame, and expanding the field operators in the angular-momentum basis, the Hamiltonian of the system takes the form

$$\hat{H} = E_0 \sum_k (k - \omega)^2 \hat{b}_k^\dagger \hat{b}_k + \frac{\epsilon}{2} \sum_k \left( \hat{b}_{k+1}^\dagger \hat{b}_k + h.c. \right) + \frac{U}{2L} \sum_{k_1, k_2, k_3, k_4} \hat{b}_{k_1}^\dagger \hat{b}_{k_2}^\dagger \hat{b}_{k_3} \hat{b}_{-k_3-k_2-k_1}, \quad (9)$$

We are interested in the time evolution with initial condition given by the nonrotating ground state (yrast state with  $l = 0$ ). The yrast states have definite angular momentum for  $\epsilon = 0$  and, within the validity of the two-mode approximation, they are given by

$$|\psi_l\rangle = (\hat{b}_0^\dagger)^{N-l} (\hat{b}_1^\dagger)^l |\text{vac}\rangle. \quad (10)$$

Truncating the Fock basis to the states (10), the Hamiltonian (9) is a tri-diagonal  $(N+1) \times (N+1)$  matrix. Fig. 2(c) shows the spectrum of this matrix for  $N = 10$ ,  $\gamma = 0.8E_0$ ,  $\epsilon = 0$ , and  $0 \leq \omega \leq 1$ . Note that for  $U = 0$  all levels would cross at one point at  $\omega = 1/2$ . Finite interactions remove this degeneracy, leading to the appearance of a caustic in the level crossing pattern. The spectrum of the system for a finite  $\epsilon = 0.04E_0$  is shown in Fig. 2(d) [15]. Now all level crossings are substituted by avoided crossings. The quantum Hamiltonian in the two mode model can be recast to take the form of a quantized version of the effective Hamiltonian (3), where the action variable  $I$  is now associated with the operator  $\hat{I} = -i(1/N)\partial/\partial\theta$  and  $1/N$  plays the role of the Planck constant. In particular, we find that the transition frequency between the caustic levels is given by  $\Omega_s$  of Eq. (5).

The quantum analysis also helps us to identify a condition for the frequency  $\omega_{max}$ . The positions of the lowest two levels in Fig. 2(c) for  $\omega = 0$  are  $E_1(\omega) = E_1(0) + NE_0\omega^2$  and  $E_2(\omega) = E_2(0) + NE_0\omega^2 - 2E_0\omega$ , respectively, with  $E_1(0) = N\gamma/2$  and  $E_2(0) = E_0 + (N/2 + 1)\gamma$ . Setting  $E_1(\omega) = E_2(\omega)$  we obtain

$$\omega_{max} \approx \frac{1}{2} + \frac{\gamma}{2E_0}, \quad \gamma \ll E_0. \quad (11)$$

For the parameters of Fig. 2,  $\omega_{max} \approx 0.87$ . A more thorough comparison of the upper and lower rows in Fig. 2 indicates that energies of the soliton states calculated within the mean-field approximation are shifted in the negative direction compared to the quantum calculation. This is a manifestation of the occupation of additional angular momentum modes outside the two-mode model. We also note that in the semiclassical limit  $N \rightarrow \infty$  the energy difference between the ground ( $l = 0$ ) and excited ( $l > 0$ ) vortex states for  $\omega = 0$  is given by the Bogoliubov result:  $\hbar\Omega_l = \sqrt{(lE_0)^2 + 2E_0\gamma}$ . This generalizes Eq. (11) for the critical frequency  $\omega_{max}$  as  $\omega_{max} = \hbar\Omega_1/2E_0$ . It is easy to see that this coincides

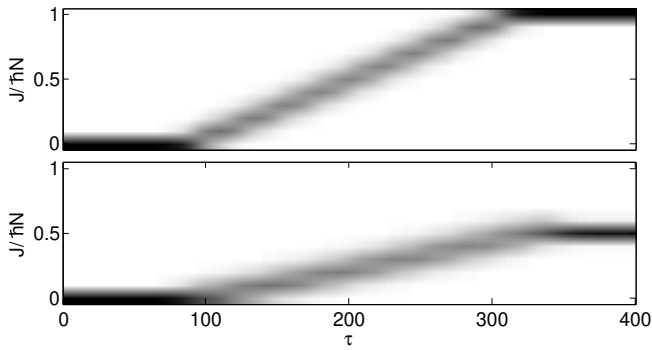


FIG. 3. Adiabatic passage from the ground state to the yrast states  $|\psi_N\rangle$  (upper panel) and  $|\psi_{N/2}\rangle$  (lower panel). The parameters are the same as in Fig. 1.

with (11) in the limit  $\gamma \ll E_0$ . Generally, it looks possible to excite the vortex state with topological charge  $l$  through metastable states with  $l$  dark solitons [5] by choosing  $\hbar\Omega_l/2E_0 < \omega_{max} < \hbar\Omega_{l+1}/2E_0$  [17].

It is interesting to simulate the dynamics of the quantum system (9) for the same protocols as were used in the mean-field simulations. Due to exponential proliferation of the Hilbert space with  $N$ , this can be done only for small number of atoms  $N \sim 10$ . Fig. 3 shows the dynamics of the system (9) in the two-mode approximation for  $N = 10$  and  $\gamma = 0.8E_0$ . (We have checked that for these value of the interaction constant and number of particles the result remains unchanged if we use a four-mode approximation.) The gray-color scale encodes populations of the Fock states (10). It is seen in Fig. 3 that our protocols almost entirely populate the target yrast state  $|\psi_N\rangle$  (upper panel) and  $|\psi_{N/2}\rangle$  (lower panel), respectively, with the probabilities 0.98 and 0.93.

The quantum model (10) reveals why global symmetry breaking is effective for nucleating the metastable phase transition: The long wavelength, symmetry breaking potential proportional to  $\epsilon$  couples neighboring yrast states (11) effectively and thus creates the avoided crossings that provide the adiabatic passage. There is still a crucial difference between the quantum and mean field models: While the soliton states of the GP approximation break the rotational symmetry, the corresponding yrast states (11) do not. Instead, they correspond to fragmented condensates, where both the occupation of the  $k = 0$  and the  $k = 1$  mode can become large. Whether we obtain a fragmented condensate with preserved rotational symmetry or a condensate with broken symmetry, depends on the rate for changing the parameter  $\epsilon$  at the very end of the passage, where  $\epsilon < \epsilon_{cr} \sim E_0/N$ . For large  $N$  it becomes more difficult to restore symmetry since for  $\epsilon \rightarrow 0$  the system ‘sits’ on the caustic, where the density of states tends to infinity if  $N \rightarrow \infty$ .

So far we have considered the case of moderate nonlinearity, where the two-mode approximation is justified.

In typical experiments with BECs, larger nonlinearities beyond the validity of the two-mode approximation are relevant. We have verified within the mean-field theory that adiabatic passage for stronger nonlinearities is possible as well [17]. In this case  $\Omega_{max} - \Omega_{min} \approx \hbar^{-1} \sqrt{E_0 \gamma / 2}$ . By using Eq. (8) and setting  $\epsilon \sim \gamma$ , the time scales for the adiabatic change can be estimated as  $\Delta t \gg mR^2/\hbar$ . In the recent experiment with  $^{23}\text{Na}$  [16],  $R \sim 20\mu\text{m}$ . This gives  $\Delta t \gg 1\text{s}$ . For lighter atoms, e.g.  $^7\text{Li}$ , and smaller radius, e.g.  $R \sim 10\mu\text{m}$ , one can achieve the condition  $\Delta t \gg 0.1\text{s}$  and  $\theta \approx 0.5^\circ$ . Therefore, the time scales of the order of 1s will provide the adiabatic passage.

In conclusion, we have proposed an experimental scheme to nucleate a metastable quantum phase transition in an ultra-cold Bose gas by an adiabatic passage. We have shown that this is achieved by an explicit breaking of the global rotational symmetry. The procedure generalizes nucleation procedures, which change the ground state symmetries in the course of ordinary continuous phase transitions. The proposed scheme can be used to generate dark solitons and persistent ring currents with desired angular momentum.

We acknowledge stimulating discussions with Jean-Sebasti  n Caux and Lincoln Carr. AK thanks Massey University for hospitality. OF, MCD and JB were supported by the Marsden Fund (contract No. MAU0910) administrated by the Royal Society of New Zealand.

- 
- [1] W.H. Zurek, *Nature* **317**, 505 (1985); R.D. Averitt, *Nature Phys.* **6** 639 (2010); R. Yusupov *et al.*, *ibid.* **6**, 681 (2010)
  - [2] L.D. Carr, *Understanding Quantum Phase Transitions* (Taylor and Francis, 2010).
  - [3] M.A. Caprio, P. Cejnar, F. Iachello, *Ann. Phys.* **323**, 1106 (2008).
  - [4] V. S. Shchesnovich and V. V. Konotop, *Phys. Rev. Lett.* **102**, 055702 (2009).
  - [5] R. Kanamoto, L.D. Carr, and M. Ueda, *Phys. Rev. Lett.* **100**, 060401 (2008); R. Kanamoto, L.D. Carr, and M. Ueda, *Phys. Rev. A* **79**, 063616 (2009).
  - [6] S. Sachdev and B. Keimer, *Phys. Today* **64**, 29 (2011).
  - [7] D. Dagnino, N. Barberan, M. Lewenstein and J. Dalibard, *Nature Phys.* **5**, 431 (2009); A. Nunnenkamp, A. Rey and K. Burnett, *Proc. R. Soc. A* **466**, 1247 (2010).
  - [8] M. Hiller, T. Kottos and D. Cohen, *Europhys. Lett.* **82**, 40006 (2008); M. Hiller, T. Kottos and D. Cohen, *Phys. Rev. A* **78**, 013602 (2008).
  - [9] D. Hallwood and J. Brand, *Phys. Rev. A* **84**, 043620 (2011).
  - [10] A. Yu. Cherny, J.-S. Caux and J. Brand, *Phys. Rev. A* **80**, 043604 (2009).
  - [11] L. Pitaevskii and S. Stringari, *Bose-Einstein condensation* (Oxford University Press, New York, 2003).
  - [12] N.V. Vitanov, M. Fleischhauer, B.W. Shore, and K. Bergmann, *Adv. Atomic Mol. Opt. Phys.* **46**, 55 (2001).
  - [13] C. G. Broyden, *Math. Comp.* **19** (1965), 577.
  - [14] V. V. Konotop and L. Pitaevskii, *Phys. Rev. Lett.* **93**,

- 240403 (2004).
- [15] We note in passing that a similar level crossing pattern appears in the problem of the nonlinear Landau-Zener tunnelling: D. Witthaut, E. M. Graefe, and H. J. Korsch, Phys. Rev. A **73**, 063609 (2006); B. Wu and J. Liu, Phys. Rev. Lett. **96**, 020405 (2006).
- [16] A. Ramanathan, K.C. Wright, S.R. Muniz, M. Zelan, W.T. Hill, C.J. Lobb, K. Helmerson, W.D. Phillips and G.K. Campbell, Phys. Rev. Lett. **106**, 130401 (2011).
- [17] The corresponding simulations are presented at <http://ctcp.massey.ac.nz/~mqpt>.